4-18-2012

Survival motor neuron protein deficiency impairs myotube formation by altering myogenic gene expression and focal adhesion dynamics

Katherine V. Bricceno
National Institutes of Health, Bethesda, MD

Tara Martinez
Johns Hopkins University

Evgenia Leikina
National Institutes of Health, Bethesda, MD

Stephanie Duguez
Children's National Medical Center

Terence A. Partridge
George Washington University

See next page for additional authors

Authors
Katherine V. Bricceno, Tara Martinez, Evgenia Leikina, Stephanie Duguez, Terence A. Partridge, Leonid V. Chernomordik, Kenneth H. Fischbeck, Charlotte J. Sumner, and Barrington G. Burnett

HMG Advance Access published May 7, 2014

Human Molecular Genetics, 2014 **1–13**
doi:10.1093/hmg/ddu189

Survival motor neuron protein deficiency impairs myotube formation by altering myogenic gene expression and focal adhesion dynamics

Katherine V. Bricceno[1,3], Tara Martinez[4], Evgenia Leikina[2], Stephanie Duguez[6], Terence A. Partridge[6], Leonid V. Chernomordik[2], Kenneth H. Fischbeck[1], Charlotte J. Sumner[4,5] and Barrington G. Burnett[1,7,*]

[1]Neurogenetics Branch, National Institute of Neurological Disorders and Stroke and [2]Section on Membrane Biology, Program of Physical Biology, Eunice Kennedy Shriver National Institute of Child Health and Human Development, National Institutes of Health, Bethesda, MD, USA, [3]Institute of Biomedical Sciences, The George Washington University, Washington, DC, USA, [4]Department of Neurology and, [5]Department of Neuroscience, Johns Hopkins University, Baltimore, MD, USA, [6]Research Center for Genetic Medicine, Children's National Medical Center, Washington, DC, USA and [7]Department of Anatomy, Physiology and Genetics, Uniformed Services University of the Health Sciences, F. Edward Hebert School of Medicine, Bethesda, MD, USA

Received January 29, 2014; Revised and Accepted April 18, 2014

While spinal muscular atrophy (SMA) is characterized by motor neuron degeneration, it is unclear whether and how much survival motor neuron (SMN) protein deficiency in muscle contributes to the pathophysiology of the disease. There is increasing evidence from patients and SMA model organisms that SMN deficiency causes intrinsic muscle defects. Here we investigated the role of SMN in muscle development using muscle cell lines and primary myoblasts. Formation of multinucleate myotubes by SMN-deficient muscle cells is inhibited at a stage preceding plasma membrane fusion. We found increased expression and reduced induction of key muscle development factors, such as MyoD and myogenin, with differentiation of SMN-deficient cells. In addition, SMN-deficient muscle cells had impaired cell migration and altered organization of focal adhesions and the actin cytoskeleton. Partially restoring SMN inhibited the premature expression of muscle differentiation markers, corrected the cytoskeletal abnormalities and improved myoblast fusion. These findings are consistent with a role for SMN in myotube formation through effects on muscle differentiation and cell motility.

INTRODUCTION

Spinal muscular atrophy (SMA) is an autosomal recessive disease characterized by proximal muscle weakness and degeneration of anterior horn cells (1). It is caused by mutation of the *SMN1* gene and deficiency of survival motor neuron (SMN) protein (2). There is evidence to support a role for muscle in the pathophysiology of SMA. SMN co-localizes with α-actinin in myofibers, indicating a possible muscle-specific function for SMN (3,4), and SMN-deficient myoblasts have decreased fusion (5). In SMA mouse models, different fiber groups are differentially affected by SMN deficiency (6–8). Targeted knock-out experiments in mice have shown that reducing SMN in muscle results in a dystrophic phenotype that is corrected with SMN expression in muscle progenitor cells (9,10). Both SMA patients and model mice have altered development of SMN-deficient muscle (11,12). Myotubes grown from biopsies of patient muscle are smaller in size, consistent with findings from the mouse model correlating muscle weakness with fewer and smaller fibers. There is a delay in post-natal muscle development that occurs in the absence of motor neuron loss. Recent work with primary muscle cells has shown that SMN has a role in myogenesis and that normal muscle differentiation requires adequate levels of SMN (13). Importantly,

*To whom correspondence should be addressed at: 4301 Jones Bridge Road, Bethesda, MD 20814, USA. Tel: +1 3012953506; Fax: +1 3014803365; Email: bburnett@usuhs.edu

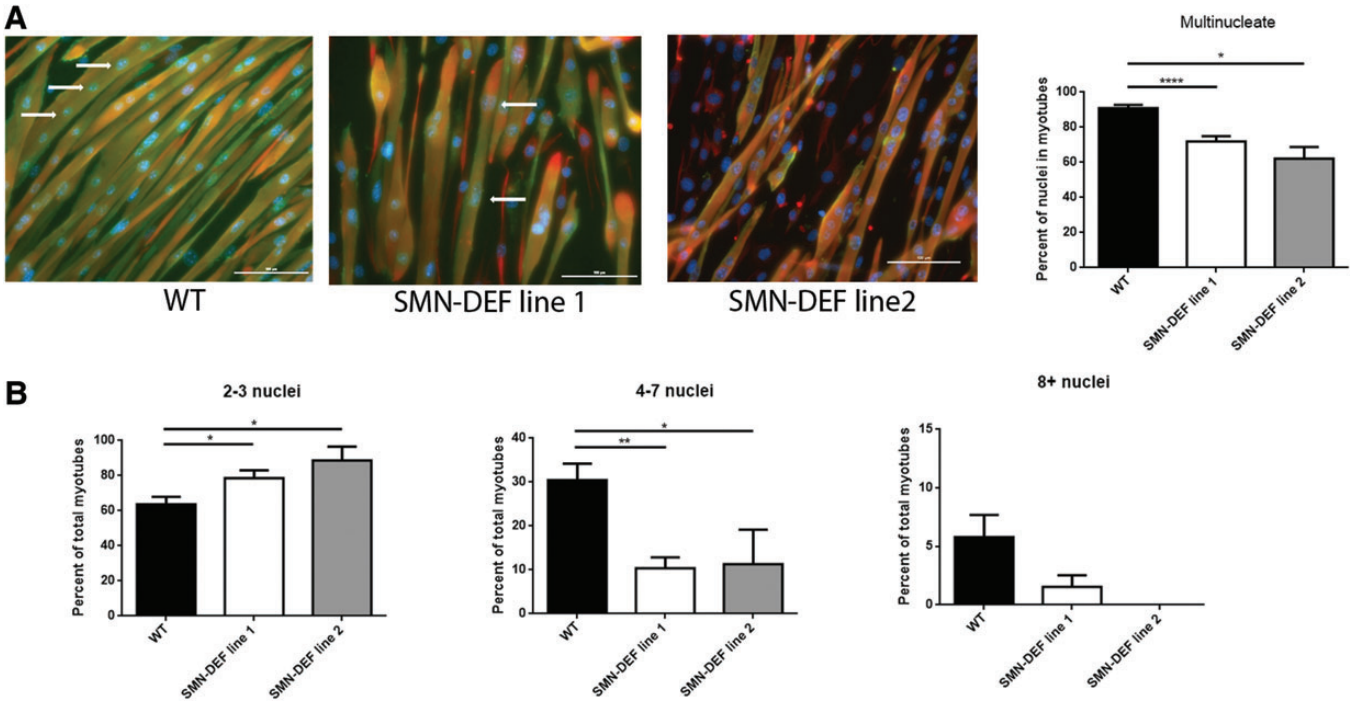

Figure 1. SMN-deficient muscle cells have a fusion deficit. Muscle cells were differentiated for 6 days and stained for sarcomeric myosin (green) and desmin (red). DAPI (blue) was added to label nuclei. Representative images are shown in (**A**). Scale bar, 100 μm. Arrows indicate myotube nuclei in each myotube. The number of nuclei in myotubes divided by the total number of nuclei in myoblasts and myotubes, the fusion index, is quantified in A. Myotubes were defined as cells positive for desmin and MF-20 with two or more nuclei. The percentage of myotubes with 2–3, 4–7 and 8 or more nuclei are quantified in (**B**). Nikon Elements software was used to count cells and nuclei. Six experiments were done per cell line. The values represent mean ± SEM ($^{*}P < 0.05$, $^{**}P < 0.01$, $^{****}P < 0.001$).

replacing SMN in SMA mouse muscle partially rescues muscle cross-sectional area and myofiber diameter (14), further supporting a role for SMN in muscle growth and development.

In normal muscle development, proliferating myoblasts differentiate, migrate and form myofibers through successive fusion events. Many factors affect the fusion process, including cell adhesion molecules, secreted molecules and their receptors, and molecules that regulate actin cytoskeleton remodeling [reviewed in (15)]. Among the cytoskeletal structures involved in myoblast fusion are focal adhesions that directly bind to the β1-integrins of the extracellular matrix (ECM) and to the actin cytoskeleton. The focal adhesion complex is made up of several proteins, including focal adhesion kinase, vinculin, α-actinin and talin (16). Altered focal adhesion dynamics disrupt cell migration and thus myoblast fusion.

In this study, we show that SMN-deficient muscle cells have a fusion deficit and altered expression of differentiation markers, which are partially rescued by restoration of SMN. We provide evidence that talin-regulated focal adhesion dynamics are disrupted and are at least in part responsible for the fusion deficit. Therefore, SMN deficiency may impair myoblast fusion through defects in differentiation and cell motility.

RESULTS

SMA muscle cell lines have a fusion deficit that is rescued by restoring SMN

It has previously been reported that SMN deficiency results in reduced myoblast fusion into multinucleated myotubes (5,13). To study the effects of SMN deficiency on myotube formation, we established muscle cell lines from an SMA model mouse. SMA delta 7 mice, which have the mouse Smn gene replaced by human *SMN2* and *SMNΔ7* (17), were crossed with mice overexpressing the H-2Kb-tsA58 (H2K) transgene (18), which encodes a thermolabile mutant of the large T antigen that allows the immortalization of the cells when grown at 33°C in the presence of γ-interferon. When muscle cells from these mice are switched to non-permissive conditions, 37°C and absence of γ-interferon, they differentiate and form myotubes. This method of generating conditionally immortal cell lines has previously been used to generate cell lines from mouse models of other muscle diseases, including limb-girdle muscular dystrophy (19). We established monoclonal cell lines of immortalized SMN-deficient (seven lines) and wild-type myoblasts (six lines) from the extensor digitorum longus (EDL) and tibialis anterior (TA) muscles of P4 pups. All lines were purified to remove fibroblasts and tested for myogenicity based on desmin staining.

Following derivation of the muscle cell lines, we confirmed that SMN levels were reduced by western blot (Supplementary Material, Fig. S1) and then sought to confirm the previous reports of a fusion deficit in SMN-deficient cells. We found reduced fusion of SMN-deficient myoblasts into multinucleate myotubes 6 days after initiating differentiation (Fig. 1A). Overall, SMN-deficient myoblasts formed myotubes with fewer nuclei (~12% of multinucleated myotubes with four or more nuclei) compared with wild-type muscle cells (35% of multinucleated myotubes with four or more nuclei) (Fig. 1B). We confirmed the fusion deficits in two SMA lines indicating

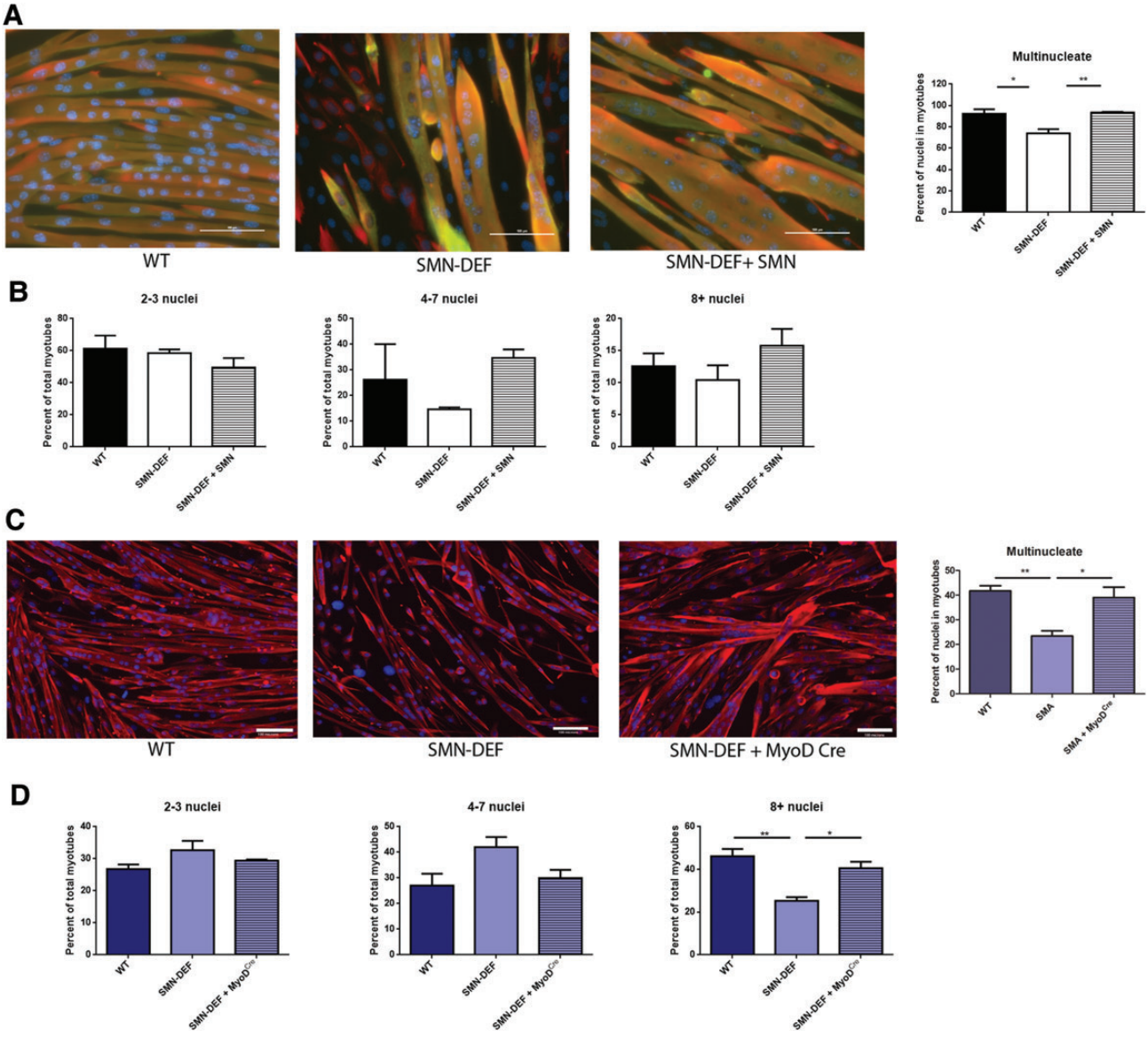

Figure 2. Restoration of SMN rescues the fusion deficit in SMN-deficient muscle cells. Electroporation was used to introduce either human *SMN* or empty vector. Muscle cells were allowed to recover in proliferation media for 6 h and then switched to differentiation conditions. The cells were differentiated for 6 days and stained for sarcomeric myosin (green) and desmin (red). DAPI (blue) was added to label nuclei. Representative images are shown in (**A**). Scale bar, 100 μm. The number of nuclei in myotubes divided by the total number of nuclei in myoblasts and myotubes, the fusion index, is quantified in A. Myotubes were defined as cells positive for desmin and MF-20 with two or more nuclei. The percentage of myotubes with 2–3, 4–7 and 8 or more nuclei are quantified in (**B**). Nikon Elements software was used to count cells and nuclei. Six experiments each were done for WT, SMN-deficient and SMN-deficient + SMN. Myoblasts were isolated from three mice each for WT, SMA and SMA + $MyoD^{Cre}$ and differentiated to myotubes for 4 days. Myotubes were stained for sarcomeric myosin (red). DAPI (blue) was added to label nuclei. Representative images are shown in (**C**). Scale bar, 100 μm. The percentage of total nuclei in myotubes is quantified in C. Myotubes were defined as cells positive for MF-20 with two or more nuclei. The percentage of myotubes with 2–3, 4–7 and 8 or more nuclei were counted by a blinded investigator and quantified in (**D**). Values represent mean ± SEM ($^{*}P < 0.05$, $^{**}P < 0.01$, $^{***}P < 0.001$).

these effects were not limited to a single clone (Fig. 1A). To establish that the fusion deficit observed in SMN-deficient myoblasts was due to reduced SMN levels, we increased levels of SMN by electroporating cDNA encoding full-length human GFP-SMN into SMN-deficient cells (Supplementary Material, Fig. S1). Assessments of GFP fluorescence showed that >90% of fibers were electroporated. Increasing SMN levels rescued the fusion deficit in the SMN-deficient cells (Fig. 2A) resulting in myotubes with numbers of nuclei approaching those of wild-type myotubes (Fig. 2B); consistent with this result, we found restoration of SMN increased the frequency of myotubes with large numbers of nuclei (Supplementary Material, Fig. S2).

We next sought to confirm our findings in primary myoblasts isolated from SMA model mice. We used conditional SMA mice that express a Cre-inducible full-length Smn allele at the mouse Smn locus with or without a Cre transgene controlled by the MyoD promoter ($Smn^{Res}MyoD^{Cre}$) (14). The MyoD-Cre transgene allows expression of full-length SMN specifically in muscle progenitor cells and myofibers (Supplementary Material, Fig. S3). The Cre-positive mice have been shown to have

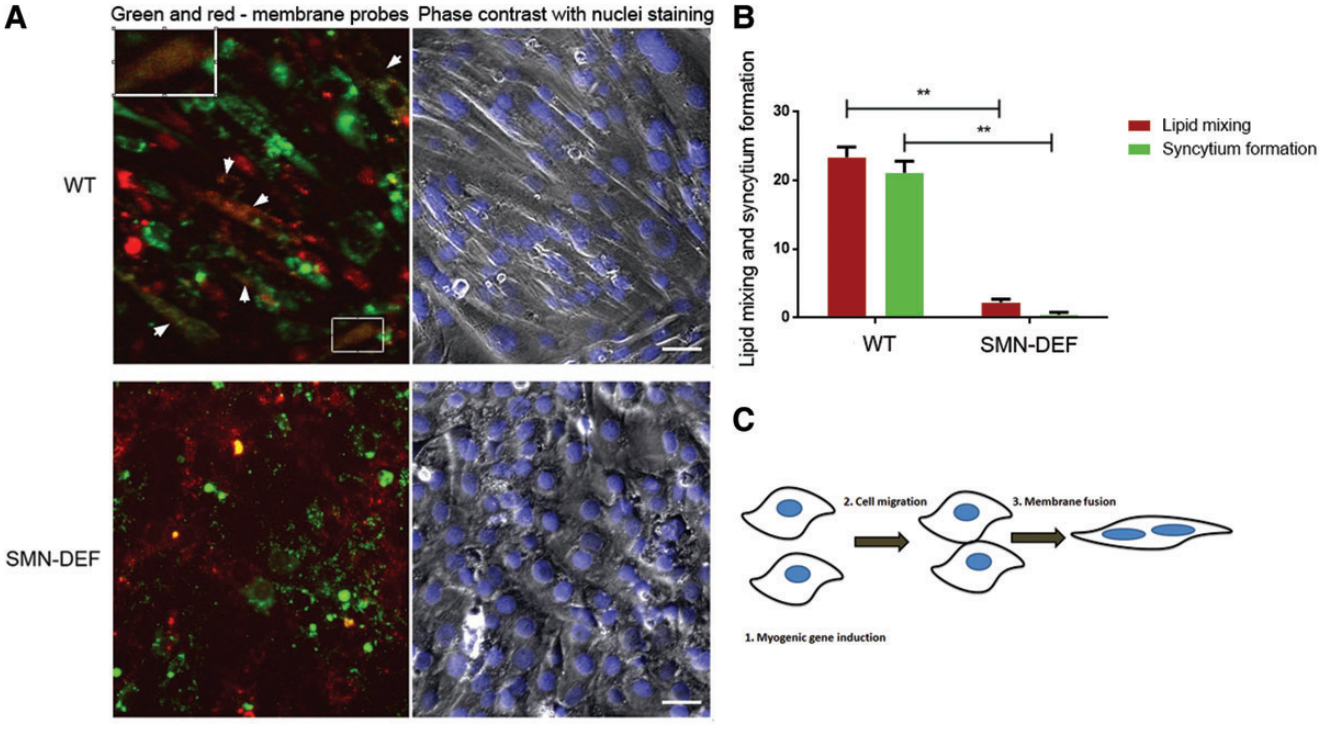

Figure 3. SMN deficiency inhibits both lipid mixing (cell-to-cell redistribution of membrane probes) and syncytium (myotube) formation. The syncytium formation assay reports only completed fusion events. In contrast, an appearance of co-labeled cells after co-incubation of differently labeled cells reveals even cell fusion events stalled upstream of generation of multinucleated cells. (**A**) Left panel, fluorescence microscopy images of the wild-type (WT) myoblasts (top) and SMN-deficient (SMN-deficient) myoblasts (bottom): DiI (red) and DiO (green). Arrowheads mark cells co-labeled with both membrane probes. A characteristic example of double-labeled cell is also shown in the 2-fold enlargement of boxed region (left top corner of the panel). Note that by the time we scored fusion, DiI and DiO incorporated into the plasma membrane are mostly internalized and label intracellular membranes. Right panel, phase contrast with nuclear staining (blue) images of the same cells. Scale bar, 40 μm. (**B**) Fusion extents for the cells expressing SMN and for the SMN-deficient cells assayed as lipid mixing (red) and as syncytium formation (green). All results are shown as mean ± SEM ($n > 3$) ($^{**}P < 0.01$). (**C**) Schematic of the sequence of events leading to myotube formation. SMN-deficient cells do not reach the third stage of the myogenesis.

full-length SMN mRNA and protein expression in muscle. We cultured primary myoblasts from leg muscles of Cre-negative and Cre-positive mice at P10. Using qRT-PCR, we verified that full-length SMN levels were reduced in the Cre-negative cells compared with wild-type cells and that the SMN levels were corrected in Cre-positive cells as expected. We next evaluated the ability of these primary myoblasts to fuse into multinucleate myotubes and determined that, as with the immortalized SMN-deficient cell lines, there was a reduced number of multinucleated myotubes in myoblasts from SMA MyoD^{Cre}-negative mice compared with WT mice. However, myoblast fusion was substantially improved in SMA mice expressing MyoD^{Cre}, with a number of nuclei per myotube similar to wild-type myoblasts (Fig. 2C and D). Together these findings indicate that SMN plays a role in myoblast fusion.

The local merger between myoblast plasma membranes and subsequent expansion of nascent fusion connections are two stages of myoblast fusion that are controlled by distinct protein machineries (20). To test whether SMN deficiency blocks myotube formation downstream from membrane merger, we co-plated myoblasts labeled with the membrane probe DiO and myoblasts labeled with membrane probe DiI in differentiation conditions. Merger of the membranes of differently labeled cells generates co-labeled cells. As expected, for wild-type myoblasts, we observed the appearance of multinucleated and co-labeled cells (Fig. 3A and B; arrowheads mark cells co-labeled with both membrane probes). In contrast, in the case of SMN-deficient myoblasts, we observed neither syncytium formation nor co-labeled cells. This finding indicates that the lack of SMN inhibits myotube formation upstream of even the earliest stages of myoblast fusion (schematic, Fig. 3C).

Proliferating SMA muscle cells have decreased expression of Pax7 and increased expression of MyoD and myogenin

Given the reduced fusion of SMN-deficient myoblasts to form multinucleate myotubes, we sought to determine the effects of SMN deficiency on myoblast differentiation. Thus, we examined the levels of markers of muscle differentiation in SMN-deficient cells compared with wild-type controls. First, we investigated the expression levels of Pax7, a muscle progenitor cell marker; MyoD and myogenin, early differentiation markers; and myosin heavy chain (MHC), a terminal muscle differentiation marker in undifferentiated, proliferating cells. Pax7 levels were reduced, whereas MyoD and myogenin levels were elevated in the SMN-deficient cells compared with wild-type cells (Fig. 4A and Supplementary Material, Fig. S4A). In addition, we found premature expression of MHC in SMN-deficient cells. These data are consistent with a previous report that SMN-deficient cells show premature muscle differentiation (13). Increasing SMN levels in SMN-deficient myoblasts restored MyoD and myogenin expression to wild-type levels

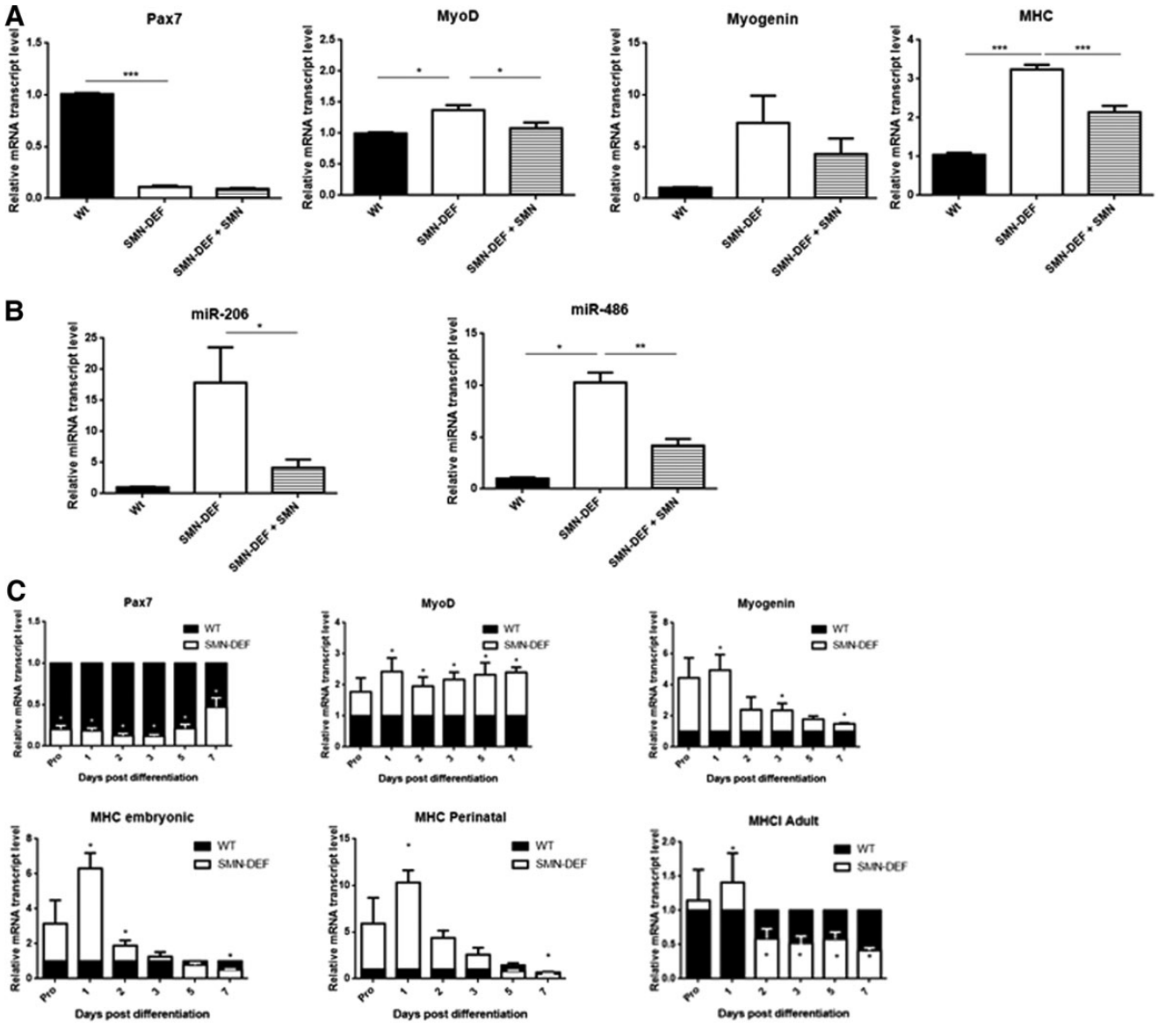

Figure 4. SMN-deficient muscle cells have increased expression of differentiation markers. (**A**) Proliferating muscle cells were collected and RNA isolated for qRT-PCR following transfection with SMN or empty vector. (**B**) qRT-PCR analysis of miR-206 and -486 expression in proliferating wild-type and SMN-deficient myoblast. (**C**) qRT-PCR following transfection with SMN or empty vector. Five time courses per genotype were run. The data are represented as the fold change compared with wild type (black bars). Four time courses per genotype were run. Values represent mean ± SEM (*$P < 0.05$, **$P < 0.01$, ***$P < 0.001$).

but had no apparent effect on Pax7 expression (Fig. 4C and Supplementary Material, Fig. S4A). During myoblast differentiation, MyoD helps to induce expression of miR-206 and -486, which further accelerate differentiation (21). Inhibition of these microRNAs causes myoblasts to remain in a proliferative state thus stalling differentiation. As we observed that MyoD expression is modulated by SMN, we next examined the expression of miR-206 and -486 in wild-type and SMN-deficient myoblasts. Compared with wild-type myoblasts, the expression of miR-206 and -486 was at least 9-fold higher in SMN-deficient cells (Fig. 4B) but restored to wild-type levels after transient transfection with SMN.

We next examined the change in expression of muscle differentiation markers over 7 days following the initiation of differentiation in SMN-deficient and wild-type cells. We found that Pax7 levels remained lower in SMN-deficient cells compared with levels in wild-type cells (Fig. 4C). Also, MyoD and myogenin expression was elevated compared with wild-type cells throughout differentiation. However, although MHC levels were prematurely elevated in SMN-deficient cells, the embryonic, perinatal and adult isoforms of MHC were significantly reduced ($P < 0.05$) at Day 7, as the cells approached terminal differentiation stage (Fig. 4C). Pax7 decreased once differentiation began, consistent with its role as a progenitor cell marker, and it was similarly reduced in the SMN-deficient and wild-type cell lines over the course of differentiation (Supplementary Material, Fig. S4B). The expression of MyoD and myogenin peaked in both SMA and wild-type cell lines after 2 days of

differentiation, but induction was lower in SMN-deficient cells compared with wild-type cells (Supplementary Material, Fig. S4B). Given the reduced induction of these early markers of muscle differentiation, we sought to determine whether MHC was also reduced. The level of induction of MHC was similar in the SMN-deficient and wild-type cell lines for the first 2 days of differentiation, after which MHC expression continued to increase in wild-type cells but remained unchanged in SMN-deficient cells (Supplementary Material, Fig. S4B). Importantly, by 7 days of differentiation, SMN-deficient myoblasts have dramatically reduced expression of terminal differentiation markers, which fits with the observed fusion deficit.

SMA muscle cells have reduced motility and altered actin cytoskeleton

To differentiate and fuse, proliferating myoblasts and satellite cells must migrate, align and establish stable cell–cell contacts. Cell migration is thus a fundamental cellular function during skeletal muscle development. We investigated whether altered cytoskeletal dynamics and cell migration contribute to the fusion deficit observed in SMN-deficient cells. To determine whether SMN deficiency affects muscle cell migration, we examined cell motility by clearing an area of cultured myoblasts and counting the number of cells migrating into the denuded region after 24 h. We found that 75% fewer SMN-deficient cells migrated into the denuded region compared with wild-type cells, indicating that cell migration is compromised (Fig. 5A). Restoration of SMN resulted in improved migration with twice the number of cells migrating into the denuded region.

Cell migration is a result of a number of molecular and cellular events, with reorganization of the actin cytoskeleton foremost among them (22). Cell spreading and migration are driven by actin polymerization and the presence of actin stress fibers. Given the reduced cell migration of SMN-deficient cells, we explored whether the actin cytoskeleton is altered in these cells. We plated myoblasts on chamber slides and observed the cytoskeleton with fluorescence microscopy, using Alexa Fluor 555-labeled phalloidin to visualize actin fibers. We found that SMN-deficient cells had a disorganized actin cytoskeleton with almost complete absence of central stress fibers (Fig. 5B). In addition, these cells had increased numbers of filopodia, protrusions and thin projections around the cell perimeter compared with wild-type cells (Fig. 5B, yellow arrows). Restoration of SMN resulted in fewer protrusions around the perimeter and more central stress fibers, similar to wild-type cells (Fig. 5B, white arrows).

Focal adhesions are sites of contact between the cell surface and the ECM, where the associated stress fibers terminate (23). They consist of structural proteins that link integrins to the actin cytoskeleton and signaling proteins that transduce a range of adhesion-dependent processes. Focal adhesions thus serve both structural and signaling functions. The structural role is to connect actin stress fibers to the ECM by the association of integrins with adaptor proteins such as vinculin, talin and α-actinin. Vinculin is an actin-binding protein involved in the mechanical coupling between the actin cytoskeleton and the ECM (24,25). Reduced vinculin expression results in increased cell spreading and cell migration, indicating a role for vinculin in the negative regulation of cell motility and focal adhesion turnover (26–29). Vinculin cycles between a closed, inactive state in the cytoplasm and an open, active state at focal adhesions where it stabilizes focal complexes (30).We examined the distribution of vinculin in SMN-deficient and wild-type cells by immunocytochemistry. In SMN-deficient cells, we found that vinculin is present at focal adhesions around the cell periphery (Fig. 5C), but there is decreased staining in the cell body compared with wild-type cells. These data suggest that the reduced migration of SMN-deficient cells could be due to persistence of vinculin at the cell periphery.

Cleavage of talin is reduced in SMA muscle cells

Talins 1 and 2 connect integrins to the actin cytoskeleton and are required for myoblast migration and fusion (31). Talin interacts with both focal adhesion proteins and actin filaments (16), and cleavage of talin regulates the turnover of focal adhesions. In the absence of talin cleavage, vinculin-positive focal adhesions are lost from the cell body and stabilized at the perimeter (32), as we observed in SMN-deficient cells. We thus examined talin protein cleavage by western blot analysis. We found that talin cleavage was reduced by $>50\%$ in SMN-deficient cells compared with wild-type controls (Fig. 6A). This finding prompted us to examine the turnover of enhanced green fluorescent protein (EGFP)—talin at protrusive structures in spreading muscle cells. To assess the effects of SMN deficiency on talin dynamics, we expressed talin in wild-type and SMN-deficient myoblasts. Time-lapse analysis of GFP-talin localization showed that talin persisted almost twice as long in adhesion complexes in SMN-deficient cells compared with wild-type cells (Fig. 6B and C). Together these data suggest that SMN deficiency results in reduced motility of myoblasts concomitant with reduced talin cleavage and increased persistence of talin and vinculin in focal adhesions (Fig. 6E). As constant focal adhesion assembly and disassembly are required for cell migration, these differences could account for the fusion deficit of SMN-deficient myoblasts.

DISCUSSION

In this study, we sought to answer two questions: does SMN deficiency cause a myoblast fusion deficit, and what are the molecular mechanisms underlying the change in fusion? We show that a smaller percentage of SMN-deficient myoblasts are incorporated into multinucleate myotubes, consistent with the fusion deficit reported by other groups (5,13,33). We extended these previous studies by showing that this fusion deficit can be rescued by restoring SMN, which indicates that SMN plays an important role in this cellular activity. We further demonstrate that SMN deficiency impedes the early stages of myoblast fusion before the cell membranes merge and that SMN-dependent alterations in the actin cytoskeleton and in focal adhesion dynamics may be contributing to the fusion deficit.

To better understand the mechanism behind the fusion defect in SMN-deficient cells, we looked for differences in the expression of markers of muscle differentiation. MyoD and myogenin are members of a family of muscle regulatory basic helix-loop-helix transcription factors that bind to regulatory

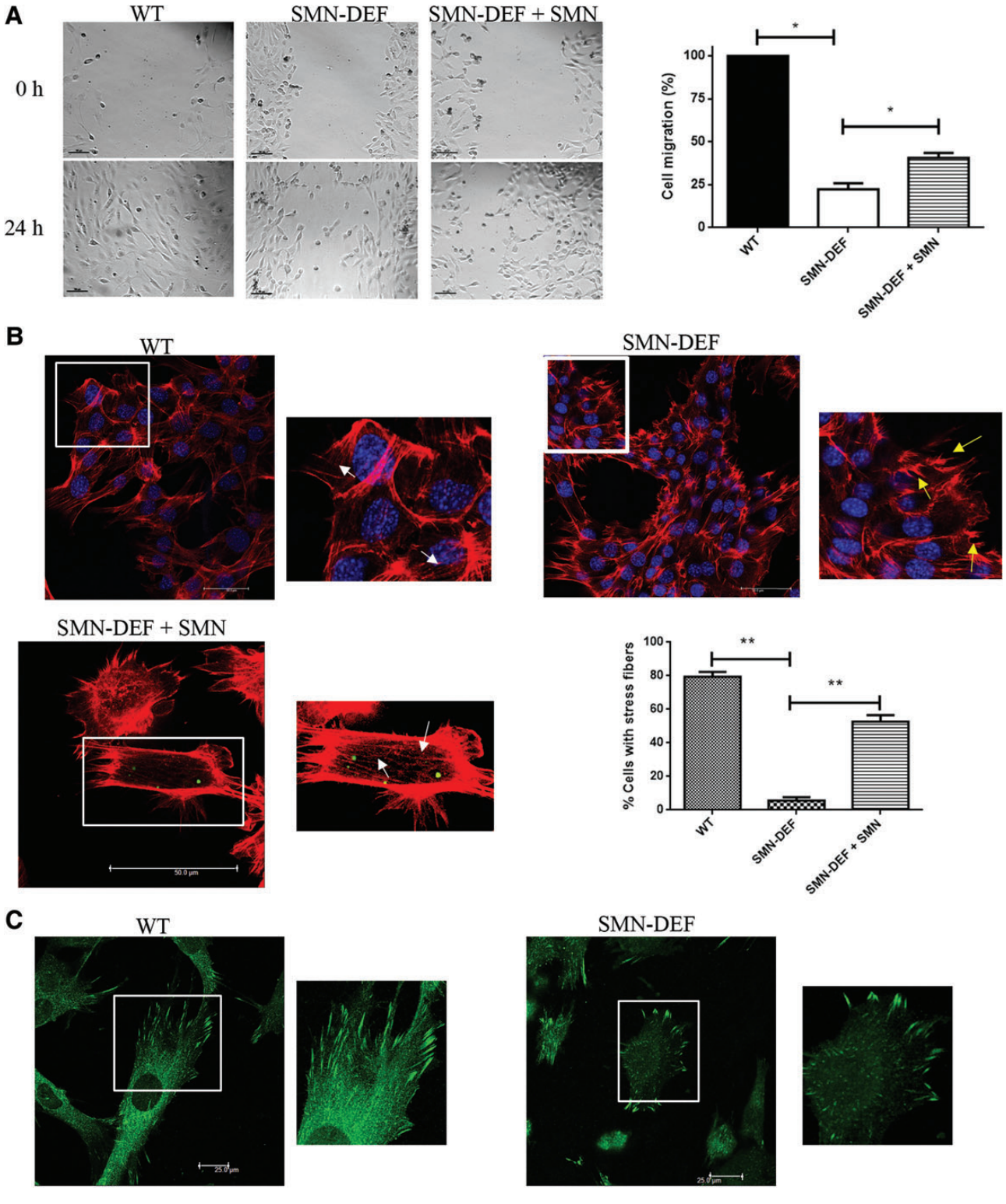

Figure 5. SMN-deficient muscle cells have altered motility and actin fiber organization. (**A**) After 1 day in differentiation conditions, confluent muscle cells were scraped off with a cell scraper and the media was replaced. The number of cells that moved into the denuded area after 24 h was counted. The data represent the average of at least three fields per experiment from four experiments. The data are shown as percentages of the wild-type average. Representative images are shown at left. (**B**) Representative images of undifferentiated muscle cells stained for F-actin (red) showing protrusions (yellow arrows) and stress fibers (white arrows). Muscle cells were transfected with GFP-SMN (green) and stained for F-actin (red). At least 50 cells per condition were counted for the presence of central stress fibers and percent cells with at least one central fiber calculated and graphed. (**C**) Representative images of undifferentiated muscle cells were stained for vinculin (green). Smaller panels are magnified images of adhesions. The values represent mean ± SEM ($^{*}P < 0.05$, $^{**}P < 0.01$, $^{***}P < 0.001$).

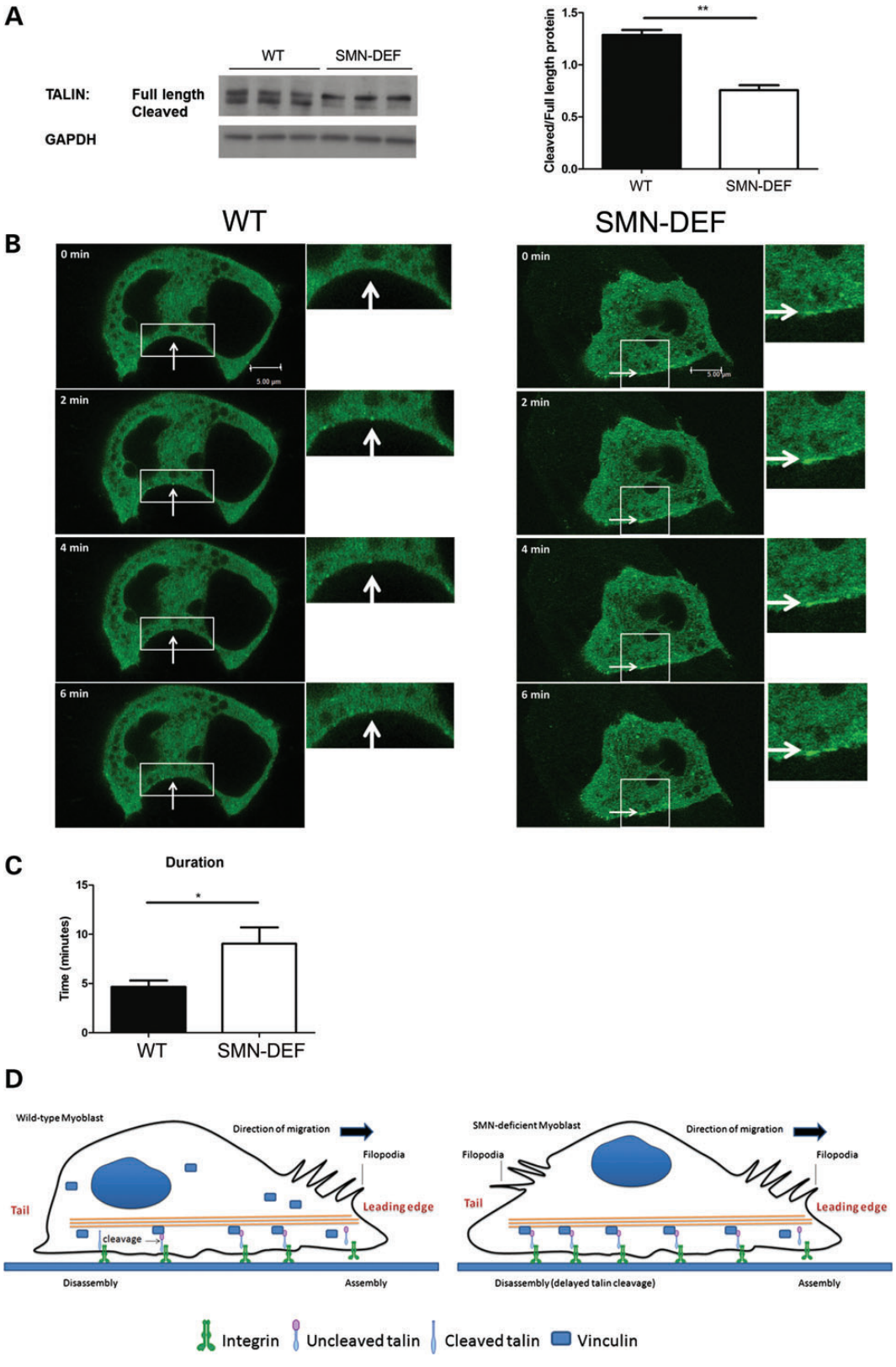

Figure 6. SMN-deficient muscle cells have decreased cleavage and increased retention of talin. (**A**) Undifferentiated muscled cells were collected and cell lysates prepared for western blot. Data are quantified as the ratio of cleaved to full-length talin. (**B**) Undifferentiated muscle cells were electroporated with human GFP-talin construct and were analyzed by time-lapse microscopy. Duration measurements were made by counting the time elapsed between the first and last frames in which an adhesion was observed. (**C**) Quantification of data in B. At least 20 adhesions were counted for each genotype. Values represent mean ± SEM ($^{*}P < 0.05$, $^{**}P < 0.01$, $^{***}P < 0.001$). (**D**) Schematic representation of proposed focal adhesion dynamics in SMN-deficient cells.

regions, E-boxes, in many genes expressed in skeletal muscle (34) and to their own regulatory sequences, creating a positive feedback loop that drives cells toward a myogenic fate (35,36). Changes in the expression or activity of these transcription factors are thus critical to muscle differentiation (35,37). The level of myogenin was higher in proliferating SMN-deficient cells, and the cells have reduced induction of this marker when switched to differentiation conditions. It is unclear whether premature expression of myogenin affects myotube formation or if the level of induction is more important than the absolute levels of myogenin. Given that SMN-deficient cells have reduced myotube formation in the presence of elevated levels of myogenin, it is possible that impaired myotube formation in SMN-deficient cell occurs because of decreased induction rather than differences in the absolute expression levels of MyoD and myogenin. Nevertheless, altered expression of these early markers of differentiation led to potentially inadequate levels of the terminal differentiation marker MHC in SMN-deficient cells, suggesting early dysregulation of muscle differentiation.

A more proximate cause of the reduced fusion of SMN-deficient myoblasts may be impairment in the transmission of mechanical forces needed for cells to migrate and fuse. The findings presented here suggest that SMN deficiency results in decreased cell migration, which could lead to a decrease in myoblast fusion. We also found that SMN-deficient myoblasts have decreased talin cleavage and retention of talin-positive focal adhesions, with increased concentration of vinculin at the cell periphery. Talin mediates the interaction between integrins and the actin cytoskeleton, and we found altered actin organization in SMA muscle cells. Focal adhesion turnover and actin dynamics are both involved in cell motility and migration, and SMN-deficient cells have altered focal adhesion dynamics and central actin fiber localization compared with wild-type cells. Overall, these data show that SMA muscle cells have SMN-dependent alterations in expression of factors critical for muscle development and cytoskeletal defects that are associated with reduced cell motility.

An increasing body of evidence suggests that SMA muscle pathology could be due in part to deficiency of SMN in muscle. *In vitro* experiments showed that SMA patient muscle can be successfully innervated with embryonic rat spinal cord explants, but the innervated myofibers undergo degeneration after 1–3 weeks; such as was not observed in cultures of muscle from aged-matched, healthy controls (38,39). Later studies showed that muscle cell lines deficient in SMN have decreased proliferation and fusion (5), and studies in mouse models of SMA found altered morphology and neuromuscular transmission (6,40,41). Together, these findings suggest that while motor neuron degeneration is characteristic of SMA, a primary deficit in muscle may be contributing to the pathology.

In a study of cell autonomy in SMA, Burghes and colleagues over-expressed SMN in striated muscle with a skeletal actin promoter and did not find a significant improvement in the lifespan of SMA model mice (42). Overexpression of SMN in neuronal cells extensively extended the lifespan of the mice. However, the muscle-specific skeletal actin promoter drives SMN expression only in post-mitotic myotubes, not proliferating myoblasts or satellite cells. If SMN indeed has a role in early muscle development, then SMN expression in proliferating cells would likely be needed to see improvement in the phenotype. Consistent with this, recent work shows that early expression of SMN in muscle tissue, driven by the MyoD promoter (active at E9.75), improves survival and motor function (14).

The phenotype of mice with muscle-specific deletion of exon 7 in murine *Smn* supports the role of SMN in muscle development. Deletion of Smn exon 7 in actively dividing muscle precursors resulted in muscle necrosis, motor paralysis and earlier death than in mice with exon 7 deleted later, in fused myotubes (9). In response to muscle damage, regeneration was impaired in mice with exon 7 deleted in muscle precursor cells and fused myotubes. In contrast, regeneration in mice with exon 7 deleted in myotubes was not significantly different from controls. Amelioration of muscle pathology in SMA may depend on correcting levels of SMN in muscle early in development.

The data presented here support a mechanism for SMN in early muscle development, specifically in regulating myogenic gene expression and actin and focal adhesion dynamics involved in cell migration. It is unclear whether the early dysregulation of myogenic programing subsequently leads to the alterations in cytoskeletal dynamics or whether these are independent events that in parallel contribute to deficits in myoblast fusion. Improved understanding of the normal function of SMN in muscle and other tissues will allow us to identify critical functions of SMN that when deficient may contribute to the SMA phenotype and therefore be targets for therapeutic intervention.

MATERIAL AND METHODS

H2K-SMA mice

Experiments were approved by the NINDS Animal Care and Use Committee. H-2Kb-tsA58 (H2K)-SMA mice were purchased from Jackson Laboratories, stock number 006553. An H2K-SMA mouse breeder colony was maintained as described in (43).

SMA MyoD^{Cre} primary myoblasts

SMA MyoD^{Cre} mice have been previously described (14). Briefly, SMA mice expressing an Smn Cre-inducible allele and two copies of SMN2 and SMNΔ7 alleles (SmnRes/SMN2+/+/ SMNΔ7+/+) were bred to MyoD^{Cre}-expressing mice. Cre-positive SMA mice were those with the inducible Smn allele in a homozygous state (SmnRes/Res/SMN2+/+/ SMNΔ7+/+) in the presence of Cre. Cre-negative SMA mice were those with the inducible Smn allele in a homozygous state (SmnRes/Res/SMN2+/+/ SMNΔ7+/+) in the absence of Cre.

Satellite cell isolation

Hind limb muscles were isolated from P10 mice and put into plain Dulbecco's Modified Eagle Medium (DMEM) in 6-well plate. The muscles were minced with a sterile razor blade and incubated at 37°C in 2 ml of 0.2% type II collagenase and displaced for 1 h 30 min into the incubation; the samples are pipetted up and down carefully to help in digestion of the muscle. After 1 h of incubation, samples were passed through a 40-μM cell strainer into a 50-ml conical tube, and 3 ml of satellite cell media was added [satellite cell media: DMEM, 5% L-glutamine, 10% FBS (Life Technologies, Grand Island, NY,

USA), 20% fetal bovine serum (Atlanta Biologicals, Lawrenceville, GA, USA) and 5% 1 × penicillin and streptomycin mixture (Life Technologies)]. The samples were centrifuged for 5 min at 1500 rpm. The supernatant was removed, and pellet was resuspended in 2.5 ml satellite cell media and plated onto one well of a 6-well plate. One hour after plating, the samples were carefully removed from the 6-well plate and re-plated on a new 6-well plate (pre-plating). Every 24 h for the next 3 days, the samples were pre-plated on a new 6-well plate. Twenty-four hours after last pre-plate, a new 6-well plate was coated with Matrigel (BD Bioscience, 1:5 dilution in plain DMEM). The samples were then plated onto coated 6-well plate for growth. Satellite cell differentiation: satellite cells were removed from 6-well plate using 0.05% trypsin for 3 min at 37°C. The cells were resuspended in 5 ml satellite cell media and centrifuged at 1500 rpm for 5 min. The pellet was resuspended in 1 ml satellite cell media, and the cells were counted using a standard hemocytometer. For differentiation, the satellite cells were plated on Matrigel-coated 96-well plates at a density of 25 000 cells per well. One hour after plating, the media was removed and replaced with differentiation media (DMEM, 5% L-glutamine, 2% FBS, 5% 1 × penicillin and streptomycin mixture) and differentiated for 4 days.

H2K-SMA cell lines

To generate H2K-SMA cell lines, P4 mice were sacrificed and myofibers were isolated from the EDL and TA muscles as described in (44). To purify the cell population, the cells were pre-plated on a Petri dish and incubated at room temperature for 20 min. Fibroblasts quickly attach to the plastic, whereas myoblasts do not attach as quickly to plastic and remain in solution. After incubation, the supernatant was transferred to a Matrigel-coated culture dish. The cells were allowed to grow (see proliferation conditions described later) until they were at least 50% confluent, and then the pre-plating process was repeated. The cells were pre-plated at least three times and then tested for myogenicity based on staining for desmin as described in (44). Once established, the muscle cell lines were maintained in proliferation media [DMEM with pyruvate and glutamine (Life Technologies), 20% FBS, 2% chick embryo extract (Accurate Chemical, Westbury, NY, USA), 20 U/ml γ-interferon (Millipore, Billerica, MA, USA), 1 × penicillin and streptomycin mixture (Life Technologies)] on culture dishes coated with Matrigel (BD Biosciences, San Jose, CA, USA) at 33°C and 10% CO_2. For differentiation into myotubes, the cells were switched to differentiation media [DMEM with pyruvate and glutamine (Life Technologies), 5% horse serum (Life Technologies), 1 × penicillin and streptomycin mixture (Life Technologies)] and cultured at 37°C and 5% CO_2.

Myoblast fusion assays

Muscle cells were grown on Matrigel-coated plastic in differentiation conditions for 6 days. The cells were fixed in 4% formalin at 37°C for 15 min, washed in phosphate-buffered saline (PBS) and blocked in 0.5% Triton X-100, 20% goat serum and 2% bovine serum albumin in Tris-buffered saline with 0.1% Triton X (TBST). The cells were immunostained with mouse anti-sarcomeric myosin (1:200; MF-20, Developmental Studies Hybridoma Bank, Iowa City, IA, USA), rabbit anti-desmin (1:200; Abcam, Cambridge, MA, USA) in 0.2% Triton X-100, 2% goat serum and 2% bovine serum albumin in TBST. Cells were washed in TBST and incubated in goat anti-mouse Alexa Fluor 488 (1:200; Life Technologies,), goat anti-rabbit Alexa Flour 555 (1:200; Life Technologies) and DAPI in the same solution as used for the primary antibodies. Following the incubations, the cells were washed in TBST. Pictures were taken with a Nikon Eclipse Ti microscope using Nikon Elements software. For the fusion index, the investigator taking the pictures did not know the genotype of the cells. Nikon Elements software was used to count cells and nuclei. Myotubes were defined as cells positive for desmin and MF-20 with two or more nuclei. The percentage of nuclei in myotubes, or fusion index, was calculated as the number of nuclei in myotubes divided by the total number of nuclei in myoblasts and myotubes.

Membrane merger assay

Cell-to-cell fusion starts with a local merger between the cell membranes. To detect fusion events in which nascent membrane connections between the cells did not expand to yield multinucleated cells, we co-plated differently labeled cells and assayed fusion as the appearance of co-labeled cells. Twenty-four hours after placement in differentiation medium, the cells were labeled as recommended by the manufacturer with one of the two fluorescent lipophilic tracers Vybrant DiI and Vybrant DiO (Molecular Probes, Inc., Eugene, OR, USA, V22885 and V-22886, respectively, 1:300 dilution). Differently labeled cells were co-plated. Fusion was scored 24 h later (20). To quantify the efficiency of myoblast fusion, we fixed the cells in phosphate-buffered, 10% w/v formalin solution (#15740; Electron Microscopy Sciences). Cell nuclei were labeled with Hoechst-33342 (Molecular Probes, Inc.). We prepared and analyzed images using Image J (National Institutes of Health). For each condition, we took images of 10 randomly chosen fields of view (greater than 600 nuclei per condition). We detected early stages of cell fusion as the redistribution of the membrane probes between differently labeled cells and presented the data as the percentage of nuclei in co-labeled cells (including both mono- and multi-nucleated cells) compared with the total number of nuclei in the field of view. The efficiency of myotube formation was quantified as the percentage of cell nuclei present in myotubes normalized to the total number of cell nuclei.

RNA isolation

Total RNA was isolated from muscle cells using Trizol (Life Technologies), and the RNeasy kit (Qiagen, Germantown, MD, USA) was used to purify the RNA according to the manufacturer's instructions (45). One microgram of RNA was converted to cDNA using the High Capacity cDNA Reverse Transcription kit (Life Technologies), following the manufacturer's instructions. Gene expression was determined by qRT-PCR using TaqMan reagents (Life Technologies). Primers were MyoD (TaqMan assay Mm00440387_m1), Myh3 (TaqMan assay Mm01332452_m1), Myh8 (TaqMan assay Mm01329494_m1), Myh7 (TaqMan assay Mm01319006_g1), Myogenin (TaqMan assay Mm00446194_m1), Pax7 (Mm00834079_m1) and Pgk1

(Mm00435617_m1). Myh3, Myh8 and Myh7 are the embryonic, perinatal and adult isoforms of MHC, respectively. Transcript levels were quantified by threshold cycle values using phosphoglycerate kinase 1 as a control. For each gene, values were normalized to unaffected cells.

Western blots

Muscle cells were lysed in 1% NP-40, 50 mM Tris–HCl (pH 8), 150 mM NaCl and protease inhibitor cocktail (Roche, Indianapolis, IN, USA) on ice for 10 min. The lysates were centrifuged at 4°C for 10 min and the supernatants collected. Protein concentration was determined using the BCA Protein Assay kit (Pierce, Rockford, IL, USA) according to the manufacturer's protocol. Protein lysates (50 μg) were resolved by SDS–PAGE (10%) and transferred to PVDF membranes. The membranes were blocked in 5% milk and probed with mouse anti-talin (1:500; clone 8d4, Sigma, St. Louis, MO, USA), rabbit anti-calpain 2 (1:1000, Cell Signaling, Danvers, MA, USA), mouse anti-GAPDH (1:4000, EnCor Biotechnology, Gainesville, FL, USA) and mouse anti-alpha tubulin (1:3000, Sigma).

Electroporation of H2K cells

DNA was transfected into H2K-SMA cells by electroporation using the Amaxa Cell Line Nucleofection Kit V (Lonza, Valais, Switzerland) following the manufacturer's instructions with the following modifications for the H2K cells. For each transfection, 500 000 cells were used. Following transfection, the cells were returned to proliferation conditions (mentioned earlier). If myotubes were required for the experiment, the cells were switched to differentiation conditions once they adhered to the dish 6 h post-electroporation. Two micrograms of GFP-SMN or GFP empty vector or GFP-talin (Addgene, Cambridge, MA, USA) was used for each transfection. For fusion assays, myc constructs described in (46) were used.

Cell migration assays

Muscle cells were grown on Matrigel-coated plastic in differentiation conditions for 1 day. An area of the well was denuded. The cells were washed in PBS and fresh media added. The cells were allowed to grow for an additional 24 h in differentiation conditions. The cells were fixed in 4% formalin at 37°C for 15 min, washed in TBST, and the number of cells that moved into the denuded area was counted. Pictures were taken with a Nikon Eclipse Ti microscope using Nikon Elements software. The investigator taking the pictures did not know the genotype of the cells.

Immunostaining

Muscle cells were grown in proliferation conditions for 2 days on glass chamber slides coated with poly-D-lysine (PDL) (Sigma). One day before plating, the slides were coated overnight at 37°C with 50 μg/ml of PDL in PBS. The next day, the slides were washed with PBS and dried for 1 h at 37°C. The slides were washed once with DMEM before plating the cells. The cells were fixed in 4% cold paraformaldehyde in PBS for 30 min at 4°C, washed in PBS and blocked in 0.3% Triton X-100 and 10% goat serum in PBS. The cells were immunostained with Alexa Fluor Phalloidin 555 (1:50, Life Technologies) or mouse anti-vinculin (1:400, Sigma) in 0.1% Triton X-100 and 5% goat serum in PBS. The cells were washed in TBST and incubated in goat anti-mouse Alexa Fluor 488 (1:200; Life Technologies) (vinculin only) and DAPI in the same solution as used for the primary antibodies. Following the incubations, the cells were washed in PBST. Pictures were taken on a Leica TCS SP5 II confocal microscope using Leica LAS AF software. The number of stress fiber per cell was determined by counting cells with at least one central stress fiber in at least 25 stained cells per condition.

Time-lapse microscopy

Time-lapse fluorescence imaging of live cells was done with a 63× objective on a Leica TCS SP5 II confocal microscope using Leica LAS AF software. The cells were transfected (mentioned earlier) with GFP-talin and grown on glass-bottom dishes coated with PDL (Sigma). One day before plating, the slides were coated overnight at 37°C with 50 μg/ml of PDL in PBS. The next day, the slides were washed with PBS and dried for 1 h at 37°C. The slides were washed once with DMEM before plating the cells. Fluorescent images were captured every 2 min for 2 h. Time-lapse sequences were used to determine the duration of focal adhesions by counting the amount of time elapsed between the first and last frame when an adhesion was observed. For each cell type, at least 20 individual adhesions were counted in five separate cells by a blinded evaluator.

Statistical analysis

Data are presented as mean ± standard error. *T*-tests were performed using GraphPad Prisim 5 software (GraphPad Software) with significance set at $P < 0.05$.

SUPPLEMENTARY MATERIAL

Supplementary Material is available at *HMG* online.

Conflict of Interest statement. None declared.

FUNDING

This work was supported by intramural NINDS research funds. B.G.B. was supported by Families of SMA. C.J.S. was supported by NINDS grant R01NS062869 and funds from the Spinal Muscular Atrophy Foundation. L.V.C. was supported by the Intramural Research Program of the Eunice Kennedy Shriver National Institute of Child Health and Human Development, National Institutes of Health.

REFERENCES

1. Park, G.H., Kariya, S. and Monani, U.R. (2010) Spinal muscular atrophy: new and emerging insights from model mice. *Curr. Neurol. Neurosci. Rep.*, **10**, 108–117.
2. Lefebvre, S., Burglen, L., Reboullet, S., Clermont, O., Burlet, P., Viollet, L., Benichou, B., Cruaud, C., Millasseau, P., Zeviani, M. *et al.* (1995) Identification and characterization of a spinal muscular atrophy-determining gene. *Cell*, **80**, 155–165.

3. Rajendra, T.K., Gonsalvez, G.B., Walker, M.P., Shpargel, K.B., Salz, H.K. and Matera, A.G. (2007) A Drosophila melanogaster model of spinal muscular atrophy reveals a function for SMN in striated muscle. *J. Cell Biol.*, **176**, 831–841.
4. Chang, H.C., Dimlich, D.N., Yokokura, T., Mukherjee, A., Kankel, M.W., Sen, A., Sridhar, V., Fulga, T.A., Hart, A.C., Van Vactor, D. *et al.* (2008) Modeling spinal muscular atrophy in Drosophila. *PLoS One*, **3**, e3209.
5. Shafey, D., Cote, P.D. and Kothary, R. (2005) Hypomorphic Smn knockdown C2C12 myoblasts reveal intrinsic defects in myoblast fusion and myotube morphology. *Exp. Cell Res.*, **311**, 49–61.
6. Murray, L.M., Comley, L.H., Thomson, D., Parkinson, N., Talbot, K. and Gillingwater, T.H. (2008) Selective vulnerability of motor neurons and dissociation of pre- and post-synaptic pathology at the neuromuscular junction in mouse models of spinal muscular atrophy. *Hum. Mol. Genet.*, **17**, 949–962.
7. Mutsaers, C.A., Wishart, T.M., Lamont, D.J., Riessland, M., Schreml, J., Comley, L.H., Murray, L.M., Parson, S.H., Lochmuller, H., Wirth, B. *et al.* (2011) Reversible molecular pathology of skeletal muscle in spinal muscular atrophy. *Hum. Mol. Genet.*, **20**, 4334–4344.
8. Monani, U.R., Sendtner, M., Coovert, D.D., Parsons, D.W., Andreassi, C., Le, T.T., Jablonka, S., Schrank, B., Rossoll, W., Prior, T.W. *et al.* (2000) The human centromeric survival motor neuron gene (SMN2) rescues embryonic lethality in Smn(-/-) mice and results in a mouse with spinal muscular atrophy. *Hum. Mol. Genet.*, **9**, 333–339.
9. Nicole, S., Desforges, B., Millet, G., Lesbordes, J., Cifuentes-Diaz, C., Vertes, D., Cao, M.L., De Backer, F., Languille, L., Roblot, N. *et al.* (2003) Intact satellite cells lead to remarkable protection against Smn gene defect in differentiated skeletal muscle. *J. Cell Biol.*, **161**, 571–582.
10. Cifuentes-Diaz, C., Frugier, T., Tiziano, F.D., Lacene, E., Roblot, N., Joshi, V., Moreau, M.H. and Melki, J. (2001) Deletion of murine SMN exon 7 directed to skeletal muscle leads to severe muscular dystrophy. *J. Cell Biol.*, **152**, 1107–1114.
11. Lee, Y.I., Mikesh, M., Smith, I., Rimer, M. and Thompson, W. (2011) Muscles in a mouse model of spinal muscular atrophy show profound defects in neuromuscular development even in the absence of failure in neuromuscular transmission or loss of motor neurons. *Dev. Biol.*, **356**, 432–444.
12. Guettier-Sigrist, S., Hugel, B., Coupin, G., Freyssinet, J.M., Poindron, P. and Warter, J.M. (2002) Possible pathogenic role of muscle cell dysfunction in motor neuron death in spinal muscular atrophy. *Muscle Nerve*, **25**, 700–708.
13. Hayhurst, M., Wagner, A.K., Cerletti, M., Wagers, A.J. and Rubin, L.L. (2012) A cell-autonomous defect in skeletal muscle satellite cells expressing low levels of survival of motor neuron protein. *Dev. Biol.*, **368**, 323–334.
14. Martinez, T.L., Kong, L., Wang, X., Osborne, M.A., Crowder, M.E., Van Meerbeke, J.P., Xu, X., Davis, C., Wooley, J., Goldhamer, D.J. *et al.* (2012) Survival motor neuron protein in motor neurons determines synaptic integrity in spinal muscular atrophy. *J. Neurosci.*, **32**, 8703–8715.
15. Abmayr, S.M. and Pavlath, G.K. (2012) Myoblast fusion: lessons from flies and mice. *Development*, **139**, 641–656.
16. Nayal, A., Webb, D.J. and Horwitz, A.F. (2004) Talin: an emerging focal point of adhesion dynamics. *Curr. Opin. Cell Biol.*, **16**, 94–98.
17. Le, T.T., Pham, L.T., Butchbach, M.E., Zhang, H.L., Monani, U.R., Coovert, D.D., Gavrilina, T.O., Xing, L., Bassell, G.J. and Burghes, A.H. (2005) SMNDelta7, the major product of the centromeric survival motor neuron (SMN2) gene, extends survival in mice with spinal muscular atrophy and associates with full-length SMN. *Hum. Mol. Genet.*, **14**, 845–857.
18. Jat, P.S., Noble, M.D., Ataliotis, P., Tanaka, Y., Yannoutsos, N., Larsen, L. and Kioussis, D. (1991) Direct derivation of conditionally immortal cell lines from an H-2Kb-tsA58 transgenic mouse. *Proc. Natl. Acad. Sci. USA*, **88**, 5096–5100.
19. Cohen, T.V., Cohen, J.E. and Partridge, T.A. (2012) Myogenesis in dysferlin-deficient myoblasts is inhibited by an intrinsic inflammatory response. *Neuromuscul. Disord.*, **22**, 648–658.
20. Leikina, E., LMellikov, K., Sanyal, S., Verma, S.K., Eun, B., Gebert, K.P., Lizunov, V.A., Kozlov, M.M. and Chernomordik, L.V. (2013) Extracellular annexins and dynamin are important for sequential steps in myoblast fusion. *J. Cell Bio.*, **200**, 109–123.
21. Dey, B.K., Gagan, J. and Dutta, A. (2011) miR-206 and -486 induce myoblast differentiation by downregulating Pax7. *Mol. Cell. Biol.*, **31**, 203–214.
22. Le Clainche, C. and Carlier, M.F. (2008) Regulation of actin assembly associated with protrusion and adhesion in cell migration. *Physiol. Rev.*, **88**, 489–513.
23. Huttenlocher, A. and Horwitz, A.R. (2011) Integrins in cell migration. *Cold Spring Harb. Perspect. Biol.*, **3**, a005074.
24. Zamir, E. and Geiger, B. (2001) Molecular complexity and dynamics of cell-matrix adhesions. *J. Cell Sci.*, **114**, 3583–3590.
25. Ziegler, W.H., Liddington, R.C. and Critchley, D.R. (2006) The structure and regulation of vinculin. *Trends Cell Biol.*, **16**, 453–460.
26. Volberg, T., Geiger, B., Kam, Z., Pankov, R., Simcha, I., Sabanay, H., Coll, J.L., Adamson, E. and Ben-Ze'ev, A. (1995) Focal adhesion formation by F9 embryonal carcinoma cells after vinculin gene disruption. *J. Cell Sci.*, **108** (Pt 6), 2253–2260.
27. Xu, W., Baribault, H. and Adamson, E.D. (1998) Vinculin knockout results in heart and brain defects during embryonic development. *Development*, **125**, 327–337.
28. Xu, W., Coll, J.L. and Adamson, E.D. (1998) Rescue of the mutant phenotype by reexpression of full-length vinculin in null F9 cells; effects on cell locomotion by domain deleted vinculin. *J. Cell Sci.*, **111** (Pt 11), 1535–1544.
29. Saunders, R.M., Holt, M.R., Jennings, L., Sutton, D.H., Barsukov, I.L., Bobkov, A., Liddington, R.C., Adamson, E.A., Dunn, G.A. and Critchley, D.R. (2006) Role of vinculin in regulating focal adhesion turnover. *Eur. J. Cell Biol.*, **85**, 487–500.
30. Chen, H., Cohen, D.M., Choudhury, D.M., Kioka, N. and Craig, S.W. (2005) Spatial distribution and functional significance of activated vinculin in living cells. *J. Cell Biol.*, **169**, 459–470.
31. Conti, F.J., Monkley, S.J., Wood, M.R., Critchley, D.R. and Muller, U. (2009) Talin 1 and 2 are required for myoblast fusion, sarcomere assembly and the maintenance of myotendinous junctions. *Development*, **136**, 3597–3606.
32. Dourdin, N., Bhatt, A.K., Dutt, P., Greer, P.A., Arthur, J.S., Elce, J.S. and Huttenlocher, A. (2001) Reduced cell migration and disruption of the actin cytoskeleton in calpain-deficient embryonic fibroblasts. *J. Biol. Chem.*, **276**, 48382–48388.
33. Arnold, A.S., Gueye, M., Guettier-Sigrist, S., Courdier-Fruh, I., Coupin, G., Poindron, P. and Gies, J.P. (2004) Reduced expression of nicotinic AChRs in myotubes from spinal muscular atrophy I patients. *Lab. Invest.*, **84**, 1271–1278.
34. Blackwell, T.K. and Weintraub, H. (1990) Differences and similarities in DNA-binding preferences of MyoD and E2A protein complexes revealed by binding site selection. *Science*, **250**, 1104–1110.
35. Brennan, T.J., Edmondson, D.G. and Olson, E.N. (1990) Aberrant regulation of MyoD1 contributes to the partially defective myogenic phenotype of BC3H1 cells. *J. Cell Biol.*, **110**, 929–937.
36. Thayer, M.J., Tapscott, S.J., Davis, R.L., Wright, W.E., Lassar, A.B. and Weintraub, H. (1989) Positive autoregulation of the myogenic determination gene MyoD1. *Cell*, **58**, 241–248.
37. Molkentin, J.D. and Olson, E.N. (1996) Defining the regulatory networks for muscle development. *Curr. Opin. Genet. Dev.*, **6**, 445–453.
38. Askanas, V., Kwan, H., Alvarez, R.B., Engel, W.K., Kobayashi, T., Martinuzzi, A. and Hawkins, E.F. (1987) De novo neuromuscular junction formation on human muscle fibres cultured in monolayer and innervated by foetal rat spinal cord: ultrastructural and ultrastructural--cytochemical studies. *J. Neurocytol.*, **16**, 523–537.
39. Guettier-Sigrist, S., Coupin, G., Braun, S., Rogovitz, D., Courdier, I., Warter, J.M. and Poindron, P. (2001) On the possible role of muscle in the pathogenesis of spinal muscular atrophy. *Fundam. Clin. Pharmacol.*, **15**, 31–40.
40. Kariya, S., Park, G.H., Maeno-Hikichi, Y., Leykekhman, O., Lutz, C., Arkovitz, M.S., Landmesser, L.T. and Monani, U.R. (2008) Reduced SMN protein impairs maturation of the neuromuscular junctions in mouse models of spinal muscular atrophy. *Hum. Mol. Genet.*, **17**, 2552–2569.
41. Kong, L., Wang, X., Choe, D.W., Polley, M., Burnett, B.G., Bosch-Marce, M., Griffin, J.W., Rich, M.M. and Sumner, C.J. (2009) Impaired synaptic vesicle release and immaturity of neuromuscular junctions in spinal muscular atrophy mice. *J. Neurosci.*, **29**, 842–851.
42. Gavrilina, T.O., McGovern, V.L., Workman, E., Crawford, T.O., Gogliotti, R.G., DiDonato, C.J., Monani, U.R., Morris, G.E. and Burghes, A.H. (2008) Neuronal SMN expression corrects spinal muscular atrophy in severe SMA mice while muscle-specific SMN expression has no phenotypic effect. *Hum. Mol. Genet.*, **17**, 1063–1075.
43. Avila, A.M., Burnett, B.G., Taye, A.A., Gabanella, F., Knight, M.A., Hartenstein, P., Cizman, Z., Di Prospero, N.A., Pellizzoni, L., Fischbeck, K.H. *et al.* (2007) Trichostatin A increases SMN expression and survival in a mouse model of spinal muscular atrophy. *J. Clin. Invest.*, **117**, 659–671.

44. Rosenblatt, J.D., Lunt, A.I., Parry, D.J. and Partridge, T.A. (1995) Culturing satellite cells from living single muscle fiber explants. *In Vitro Cell. Dev. Biol. Anim.*, **31**, 773–779.
45. Bricceno, K.V., Sampognaro, P.J., Van Meerbeke, J.P., Sumner, C.J., Fischbeck, K.H. and Burnett, B.G. (2012) Histone deacetylase inhibition suppresses myogenin-dependent atrogene activation in spinal muscular atrophy mice. *Hum. Mol. Genet.*, **21**, 4448–4459.
46. Burnett, B.G., Munoz, E., Tandon, A., Kwon, D.Y., Sumner, C.J. and Fischbeck, K.H. (2009) Regulation of SMN protein stability. *Mol. Cell. Biol.*, **29**, 1107–1115.